Testing Loop Quantum Gravity from Observational Consequences of Nonsingular Rotating Black Holes

Suddhasattwa Brahma,[1,*] Che-Yu Chen,[2,†] and Dong-han Yeom[3,4,‡]
[1]Department of Physics, McGill University, Montréal QC H3A 2T8, Canada
[2]Institute of Physics, Academia Sinica, Taipei 11529, Taiwan
[3]Department of Physics Education, Pusan National University, Busan 46241, Republic of Korea
[4]Research Center for Dielectric and Advanced Matter Physics, Pusan National University, Busan 46241, Republic of Korea

(Received 3 December 2020; revised 27 January 2021; accepted 8 April 2021; published 6 May 2021)

The lack of rotating black hole models, which are typically found in nature, in loop quantum gravity (LQG) substantially hinders the progress of testing LQG from observations. Starting with a nonrotating LQG black hole as a seed metric, we construct a rotating spacetime using the revised Newman-Janis algorithm. The rotating solution is nonsingular everywhere and it reduces to the Kerr black hole asymptotically. In different regions of the parameter space, the solution describes (1) a wormhole without event horizon (which, we show, is almost ruled out by observations), (2) a black hole with a spacelike transition surface inside the event horizon, or (3) a black hole with a timelike transition region inside the inner horizon. It is shown how fundamental parameters of LQG can be constrained by the observational implications of the shadow cast by this object. The causal structure of our solution depends crucially only on the spacelike transition surface of the nonrotating seed metric, while being agnostic about specific details of the latter, and therefore captures universal features of an effective rotating, nonsingular black hole in LQG.

DOI: 10.1103/PhysRevLett.126.181301

Introduction.—Direct detection of gravitational waves and images of black hole shadows has ushered in a golden era of black hole astronomy. At present, these extreme stellar objects serve as our best candidates for testing fundamental quantum gravity theories, such as loop quantum gravity (LQG). LQG, being a nonperturbative approach to quantum gravity, goes beyond general relativity to resolve classical singularities in cosmological and (nonrotating) black hole spacetimes and, in this Letter, we extend similar techniques to the case of the rotating Kerr-like black hole. Indeed, a consistent LQG black hole (LQGBH) model should not only provide a singularity-free description of the spacetime inside the horizon, but it must also have a viable picture for the exterior region with verifiable consequences for these observations.

Because of technical difficulties in solving the LQG equations of motion, especially when using real-valued Ashtekar-Barbero variables, axisymmetric spacetimes have remained largely unexplored. Since this is the class of spacetimes to which the Kerr black hole belongs, a direct loop quantization of rotating black holes therefore is yet to be achieved (see [1,2] for previous attempts). However, from the point of view of phenomenology, this is the primary case of interest, as most of the astrophysical black holes that have been observed are those with nonzero angular momenta.

On the other hand, LQG effective equations have been thoroughly investigated for static, spherically symmetric, and nonrotating spacetimes, resulting in quantum extensions of the Schwarzschild black hole (see [3–17] for an incomplete list of these models, [18] for a critical review, and [19,20] for signature-changing solutions). In this Letter, starting from a nonrotating LQGBH [3,4], we construct a rotating spacetime using the Newman-Janis Algorithm (NJA) [21]. As a solution-generating method, NJA is successful in constructing the Kerr (Kerr-Newman) solution from the Schwarzschild (Reissner-Nordström) black hole. We wish to follow a similar strategy for their (loop) quantum counterparts in the hope that such a solution will not only exhibit a nonsingular geometry that one expects but also tell us how LQG effects can be tested in a realistic manner. *A priori*, it might seem a little *ad hoc* to construct LQG solutions of rotating black holes in this way. However, this is similar in spirit to the "effective equations" one typically employs in symmetry-reduced models of LQG (e.g., for LQGBHs), include nonperturbative corrections inspired from the full theory. Analogously, we derive an effective rotating, singularity-free spacetime that captures key aspects of LQG.

Previous attempts at generating rotating spacetimes, using NJA, starting from a nonrotating LQGBH, suffer either from using the now outdated self-dual variables formalism [22] or an incorrect implementation of NJA [23,24]. The nonrotating LQGBH [3,4] that we are going to consider as the seed metric has several attractive features: In addition to the resolution of classical singularities as is

expected to happen in LQG, the quantum effects (quantified by a single parameter) rapidly die out when moving away from the center, with a well-defined asymptotic region in the exterior, a property not shared by all effective models of LQGBHs [25]. We will show that the rotating counterpart also retains these characteristics. However, note that our solution is more general and some of its crucial features do not depend on explicit details of the seed metric we have used, thereby capturing some universal properties of rotating LQGBHs.

As we will show, the inclusion of spin naturally enriches the spacetime structure. In particular, it is possible to generate a rotating wormhole without horizon, although this geometry is disfavored by the measurement of the shadow of M87* by the Event Horizon Telescope Collaboration (EHT) [26]. The most intriguing geometry is a regular black hole containing two horizons, with a timelike transition surface inside the inner one. Such a geometry is observationally favored by the requirement that the quantum parameter is extremely small.

Nonrotating LQGBH.—On solving the LQG effective equations, the quantum extension of the Schwarzschild metric reads [3,4]

$$ds^2 = -\tilde{a}(x)d\tau^2 + \frac{dx^2}{\tilde{a}(x)} + b(x)^2 d\Omega_2^2. \tag{1}$$

The metric functions are defined in terms of the radial variable $x \in (-\infty, \infty)$ as

$$b(x)^2 = \frac{A_\lambda}{\sqrt{1+x^2}} \frac{M_B^2 (x+\sqrt{1+x^2})^6 + M_W^2}{(x+\sqrt{1+x^2})^3}, \tag{2}$$

$$\tilde{a}(x) = \left(1 - \sqrt{\frac{1}{2A_\lambda}} \frac{1}{\sqrt{1+x^2}}\right) \frac{1+x^2}{b(x)^2}, \tag{3}$$

where M_B and M_W correspond to two Dirac observables in the model. For convenience, we have defined a dimensionless parameter $A_\lambda \equiv (\lambda_k / M_B M_W)^{2/3}/2$, where the quantum parameter λ_k originates from holonomy modifications [3,4]. In LQG, these nonperturbative corrections arise from regularizing the curvature components when considering holonomies around loops that can be shrunk only to the minimum nonzero eigenvalue of the area operator (known as the area gap), as opposed to taking the limit to zero as in classical general relativity. One of our main findings is that the quantum parameter, and thereby this fundamental "area gap," is constrained by observations of shadows of rotating black holes.

The most important feature of this LQGBH (1) is that inside the black hole, the areal radius b reaches a minimum value, representing a spacelike transition surface that smoothly connects an asymptotically Schwarzschild black hole to a white hole with mass M_B and M_W, respectively. Specifically, we will focus on the physically interesting case of the symmetric bounce in which $M_B = M_W$; i.e., the spacetimes are symmetric with respect to the transition surface ($x = 0$). Rescaling the coordinates $(x, \tau) \to (y, t)$ as $y \equiv \sqrt{8A_\lambda} M_B x$ and $t \equiv \tau/\sqrt{8A_\lambda} M_B$, the metric (1) can be rewritten as

$$ds^2 = -8A_\lambda M_B^2 \tilde{a}(y) dt^2 + \frac{dy^2}{8A_\lambda M_B^2 \tilde{a}(y)} + b(y)^2 d\Omega_2^2. \tag{4}$$

When $|y| \to \infty$, we have $|y| \to b$ and $8A_\lambda M_B^2 \tilde{a}(y) \to 1 - 2M_B/b$. Therefore, the metric (4) reduces to the Schwarzschild one in the asymptotic limit ($b \to \infty$).

Rotating LQGBH.—The rotating counterpart of (1) is obtained using NJA, in which the spin parameter a is included through a complex shift on the advanced null coordinates [21]. In particular, we use the revised NJA [27], which allows a valid representation of the resulting metric in the Boyer-Lindquist coordinate system (t, y, θ, φ). As a result, the metric of the rotating LQG compact object (rLQGO)(we use compact object instead of black hole because, as will be shown later, the resulting spacetime could be without any trapping regions, in some parts of the parameter space) can be cast in a Kerr-like form (see Supplemental Material [28] for details of the construction):

$$ds^2 = -\left(1 - \frac{2Mb}{\rho^2}\right) dt^2 - \frac{4aMb\sin^2\theta}{\rho^2} dt d\varphi + \rho^2 d\theta^2 + \frac{\rho^2 dy^2}{\Delta} + \frac{\Sigma \sin^2\theta}{\rho^2} d\varphi^2, \tag{5}$$

where $\rho^2 = b^2 + a^2\cos^2\theta$, $M = b(1 - 8A_\lambda M_B^2 \tilde{a})/2$, $\Delta = 8A_\lambda M_B^2 \tilde{a} b^2 + a^2$, and $\Sigma = (b^2 + a^2)^2 - a^2 \Delta \sin^2\theta$. Note that the functions $\tilde{a}$, b, M, and Δ are functions of y, as can be seen from Eqs. (2) and (3).

First, note that the metric (5) reduces to Kerr asymptotically for $|y| \to \infty$, recovering the expected classical limit, while in the limit $a \to 0$, the static LQGBH (4) is regained. Furthermore, setting $(a, M) \to 0$ gives one the flat limit [36], satisfying an essential consistency check lacking in some quantum gravity inspired solutions [37]. Second, $\Delta = 0$ defines the event horizon of rLQGO, where the variable y_h satisfies [see Eqs. (2) and (3)]

$$\sqrt{8A_\lambda + (y_h^2/M_B^2)} = 1 \pm \sqrt{1 - (a^2/M_B^2)}, \tag{6}$$

with the plus (minus) sign indicating the outer (inner) horizon on each side of the transition surface. The expression under the radical on the rhs of Eq. (6) implies that there is a maximum spin for rLQGO: $|a| \leq M_B$, which is the same as the Kerr bound. Evidently, the spacetime structure of rLQGO strongly depends on the values of the parameters $\{a, A_\lambda\}$ under consideration. As illustrated in Fig. 1, the transition surface can either be outside the outer

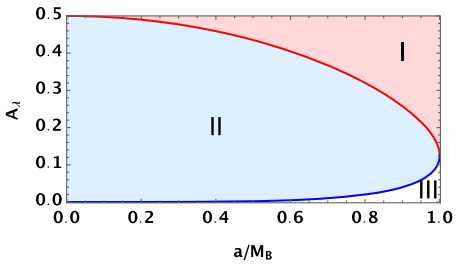

FIG. 1. The spacetime structure of the rLQGO metric (5) with respect to the parameter space $\{a, A_\lambda\}$. In regions I, II, and III, the transition surface ($y = 0$) is located outside the outer horizon, between the inner and outer horizons, and inside the inner horizon, respectively. On the red (blue) curve, the transition surface is located on the outer (inner) horizon.

horizon (region I), or between the two horizons (region II), or inside the inner horizon (region III). These regions are split by the boundaries that denote the case when the transition surface is on the outer (red curve) and the inner (blue curve) horizons.

Region I.—In this region of parameter space, the rLQGO is a rotating wormhole [Figs. 2(a) and 3(a)] without horizon. Its spacetime structure resembles that of the phenomenological Kerr-like wormhole proposed in Ref. [38]. However, the Arnowitt-Deser-Misner mass of rLQGO (5) is always M_B [28], while that of the model in Ref. [38] depends explicitly on the throat parameter. Note that the ringdown signals generated by this type of wormholes are characterized by echos [38].

Region II.—The transition surface is hidden behind the outer event horizon and becomes spacelike [Fig. 2(b)]. The green region is inside the event horizon where t and y exchange roles and the transition surface is located at the narrowest point in the middle. As expected, the Penrose diagram for this type of rotating black holes is similar to that of its nonrotating counterpart [3,4] [Fig. 3(b)], rendering the inner horizon irrelevant. This is because as $a/M_B \to 0$, the rLQGO tends to be in region II, as long as the transition surface is hidden by the outer horizon.

Region III.—Given a nonzero finite value of a/M_B, this region is characterized by a small A_λ and thus is the most physically relevant one for considering rotating black holes.

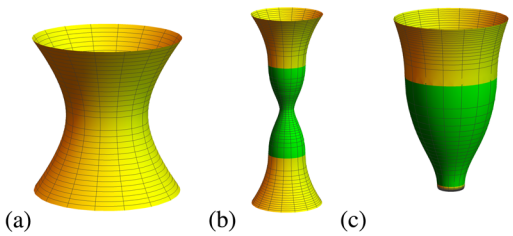

FIG. 2. The embedding diagram of rLQGO. (a) A timelike wormhole without horizon (region I). (b) A spacelike transition surface inside the event horizon (region II). (c) The transition surface is inside the inner horizon (region III).

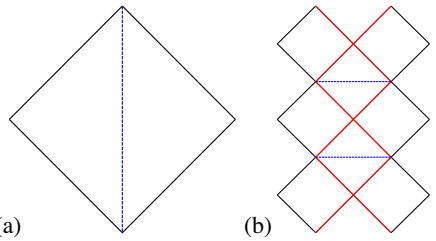

FIG. 3. The Penrose diagram of rLQGO in (a) region I and (b) region II. Blue dashed lines denote the transition surface and slanted red lines, at an angle of 45°, are event horizons.

The classical ring singularity behind the Cauchy horizon of the Kerr black hole is replaced by a timelike transition surface. As shown in its Penrose diagram (Fig. 4), a timelike trajectory (the black dashed curve) entering the black hole crosses the inner horizons (blue solid lines). Thereafter, this trajectory can be extended into another universe either by going upward (trajectory A) without touching the transition surface (blue dashed lines), or by crossing the transition surface into another interior patch (trajectory B). Its embedding diagram [Fig. 2(c)] has to terminate at a timelike surface outside the transition surface because it cannot be extended vertically downward any further (the surface of the cone becomes horizontal).

Importantly, the rLQGO is free from spacetime singularities. As shown in Fig. 5, the Ricci scalar is finite everywhere on the $(y, \cos\theta)$ plane and rapidly vanishes when moving away from the transition surface. In this figure, the solid red and blue lines represent the outer and inner horizons, respectively. The dashed curves are the ergosurface. Interestingly, because the areal radius $b \neq 0$ for rLQGO, there is no closed timelike curve that usually appears near the ring singularity inside the Kerr black hole (see Supplemental Material [28]). Even though the event horizon disappear when $|a| > M_B$, the absence of singularity naturally preserves the cosmic censorship hypothesis

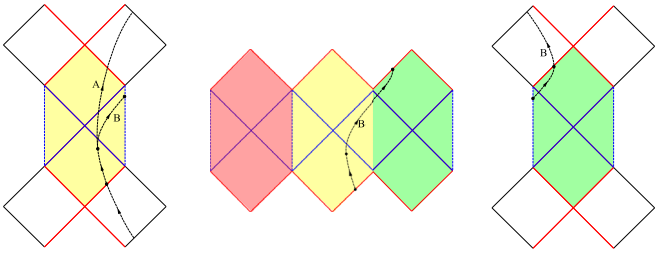

FIG. 4. The Penrose diagram of rLQGO in region III. The colored regions are inside the outer event horizon (red lines). After entering inner horizons (solid blue lines), a timelike trajectory can be extended to another universe either by going upward (trajectory A) without touching the transition surface (dashed blue lines) or by crossing the transition surface to another interior patch (trajectory B). Note that the exterior regions of the two adjacent interior patches can be causally disconnected.

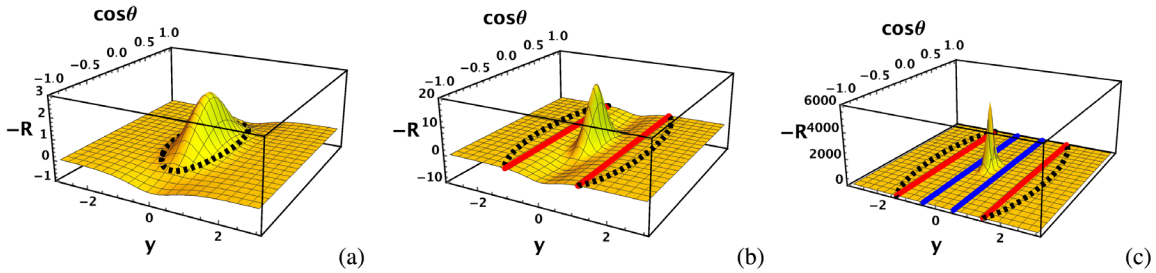

FIG. 5. The Ricci scalar R of the rLQGO spacetime expressed in the $(y, \cos\theta)$ plane. In the figure, we set $M_B = 1$ and $a/M_B = 0.9$. The solid red and blue lines represent the outer and the inner event horizons, respectively. The dashed curves represent the ergosurface. (a) A wormhole without horizon (region I with $A_\lambda = 0.4$). (b) The transition surface is covered by the outer horizon (region II with $A_\lambda = 0.1$) (c) The transition surface is inside the inner horizon (region III with $A_\lambda = 0.01$).

and the configuration looks like a "naked bounce" (similar to the rLQGO solution in region I).

Astrophysical implications.—In addition to having properties of, e.g., asymptotic flatness and regularity, we find that both the geodesic equations and the Klein-Gordon equation of the rLQGO allow for a complete separation of variables [28], following the criteria of Refs. [39,40]. The separability of the geodesic equations is useful in testing the rLQGO spacetime with its shadow and the orbital motion of surrounding particles while the separability of the Klein-Gordon equation is helpful for studying the scattering problem and the quasinormal modes [41].

As an example, let us demonstrate that it is possible, in principle, to constrain the quantum parameter A_λ using the shadow image cast by the M87*. In particular, we find that the effects made by the parameter A_λ on the shadow size R_S/M_B are more significant than those on the noncircularity of the shadow contour. Provided that the shadow size cast by M87* is consistent with that of Kerr black hole within 17% at 1σ level [42,43], one can see from Fig. 6 that the parameter space corresponding to the wormhole geometry (the region on the right of the red curve) is disfavored by the bound from the R_S measurement (black curve). Because the quantum parameter that enters the effective

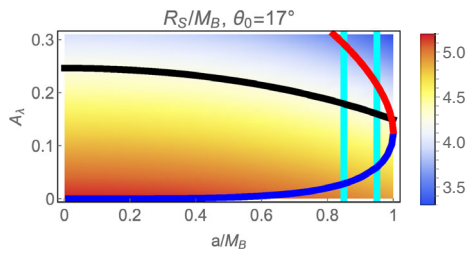

FIG. 6. The apparent size R_S/M_B of the shadow cast by rLQGO is shown with respect to the parameter space $\{a, A_\lambda\}$. The 17% bound of R_S/M_B (black curve) inferred from the M87* shadow disfavors parameters corresponding to the wormhole geometry (the region to the right of the red curve). Here we have taken into account the spin measurement obtained using the radio intensity data [45] (cyan lines) and the inclination angle measured by the jet direction [46].

equations in LQG is directly related to the fundamental area gap in the theory, shadows of rotating black holes give us a new way to constrain this parameter from observations. (Note that the quantum parameter is more tightly constrained by Solar System tests, $A_\lambda < 7.7 \times 10^{-5}$ [44]. However, this assumes the validity of Birkhoff's theorem, which need not hold in LQG.) This paves a novel method for deriving state-of-the-art constraints on LQG by examining observational consequences of rLQGO [41].

Universal features.—The most obvious limitation of our approach is that the resulting rLQGO metric is not derived by a direct loop quantization of the Kerr (or, more generally, axisymmetric) spacetime. How much of our results do we expect to generalize to such a scenario, and not be tied to the seed metric that we have chosen? First, note that the existence of a spacelike transition surface is very common for nonrotating LQGBHs, irrespective of quantization ambiguities (such as choosing the μ_0 or the $\bar{\mu}$ scheme). As this is the most crucial feature of the seed metric we have used in our construction, it is natural to expect that our rLQGO solution correctly captures the effective spacetime description of rotating LQGBHs, as long as we expect LQG to provide singularity resolution of rotating black holes in a way such that there is a smooth bouncing geometry bridging black and white holes. Furthermore, our results indicate that such a geometry observationally favors having the transition surface inside the inner horizon and is automatically consistent with the expectation that the quantum parameter is small (it inherits this property from the tiny area gap $\propto \ell_{\rm Pl}^2$). Interestingly, observations also seem to rule out models of nonrotating LQGBH spacetimes that describe a bounce outside the event horizon [47], since their rotating counterparts are at odds with observations, as well as prefer nonrotating models that allow for an inner horizon [6,8].

To make our point more explicit, we present the result of the NJA analyses on another nonrotating LQG metric proposed in [6,7] (see [28,41] for details). In Fig. 7, we show the apparent size R_S/M_B of the shadow cast by the rotating metric, which is obtained from [6,7] using NJA, in the parameter space of $\{a, \tilde{\Delta}\}$. First, we note that the spin

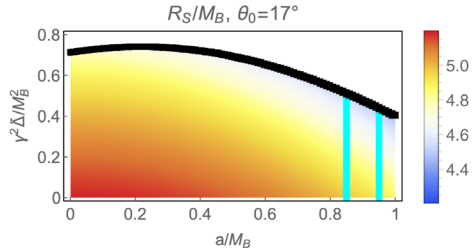

FIG. 7. The apparent size R_S/M_B of the shadow cast by the rotating black hole metric, corresponding to [6,7], in the parameter space of $\{a, \tilde{\Delta}\}$. The black boundary represents a spin-dependent upper bound of the quantum parameter, above which shadow contours disappear.

and the quantum parameter $\tilde{\Delta}$ both shrink the shadow size, exactly similar to the rLQGO case. Second, the black boundary represents a spin-dependent upper bound of the quantum parameter, above which the object cannot cast shadows. In the nonrotating limit, this upper bound can be explicitly derived as $\gamma^2\tilde{\Delta}/M_B^2 < 3^6/2^{10} \approx 0.71$, where γ is the Immirzi parameter and $\tilde{\Delta}$ is the area gap in LQG that is directly constrained in this model. Thus, we find other models of regular LQGBHs also support our general finding that the area gap is constrained to be small from observations.

Discussion.—The construction of rotating LQGBHs from holonomy-corrected effective equations in LQG is still an open problem. To catch up with the rapidly developing astronomical observations of spinning black holes in the coming years, there is an urgent need for a model of rotating LQGBHs. To derive this, an alternate path is to use a viable solution-generating method to generate a rotating solution from a nonrotating LQGBH seed metric. The resulting rLQGO spacetime (5), based on the seed metric [3,4], possesses a rather simple expression and has several interesting properties. It is everywhere nonsingular and reduces to Kerr solution asymptotically. The geodesic equations and the Klein-Gordon equation both allow complete separations of variables. Most importantly, as in the static LQGBH, the rLQGO is characterized by the existence of a transition surface induced from nonperturbative quantum corrections. Depending on the relative location of the transition surface with respect to the two horizons, the rLQGO can represent a wormhole, a regular black hole with an interior spacelike transition surface, or a regular black hole with a timelike transition region inside the inner horizon. We show that the possibility of rLQGO being a wormhole without horizon has been almost ruled out by the shadow size of M87* measured by EHT.

Most significantly, our work fills a lacuna between theoretical quantum gravity extensions of black holes, which have been mostly applied to nonrotating spacetimes, and experimental observations that have been of spinning black holes. Remarkably, we find that not only is it possible to find a regular effective description of rotating black holes from LQG, but also that an extension to such backgrounds leads to observable effects that can rule out some proposals of loop quantization for nonrotating black holes while providing support for other more generic ones that capture some universal features of LQG.

S. B. is supported in part by the NSERC (funding Reference No. CITA 490888-16) through a CITA National Fellowship and by a McGill Space Institute fellowship. C. Y. C. is supported by Institute of Physics in Academia Sinica, Taiwan. D. Y. is supported by the National Research Foundation of Korea (Grant No. 2018R1D1A1B07049126).

*suddhasattwa.brahma@gmail.com
†b97202056@gmail.com
‡innocent.yeom@gmail.com

[1] R. Gambini, E. Mato, and J. Pullin, Classical Quantum Gravity **37**, 115010 (2020).
[2] E. Frodden, A. Perez, D. Pranzetti, and C. Röken, Gen. Relativ. Gravit. **46**, 1828 (2014).
[3] N. Bodendorfer, F. M. Mele, and J. Münch, arXiv:1911.12646.
[4] N. Bodendorfer, F. M. Mele, and J. Münch, Classical Quantum Gravity **38**, 095002 (2021).
[5] R. Gambini and J. Pullin, Phys. Rev. Lett. **110**, 211301 (2013).
[6] J. G. Kelly, R. Santacruz, and E. Wilson-Ewing, Phys. Rev. D **102**, 106024 (2020).
[7] R. Gambini, J. Olmedo, and J. Pullin, Classical Quantum Gravity **37**, 205012 (2020).
[8] J. Ben Achour, F. Lamy, H. Liu, and K. Noui, Europhys. Lett. **123**, 20006 (2018).
[9] A. Ashtekar, J. Olmedo, and P. Singh, Phys. Rev. Lett. **121**, 241301 (2018).
[10] K. Blanchette, S. Das, S. Hergott, and S. Rastgoo, Phys. Rev. D **103**, 084038 (2021).
[11] E. Alesci, S. Bahrami, and D. Pranzetti, Phys. Lett. B **797**, 134908 (2019).
[12] C. Zhang, Y. Ma, S. Song, and X. Zhang, Phys. Rev. D **102**, 041502(R) (2020).
[13] F. Sartini and M. Geiller, Phys. Rev. D **103**, 066014 (2021).
[14] D. Arruga, J. Ben Achour, and K. Noui, Universe **6**, 39 (2020).
[15] M. Assanioussi, A. Dapor, and K. Liegener, Phys. Rev. D **101**, 026002 (2020).
[16] T. De Lorenzo, A. Giusti, and S. Speziale, Gen. Relativ. Gravit. **48**, 31 (2016); **48**, 111(E) (2016).
[17] J. Ben Achour, S. Brahma, S. Mukohyama, and J. P. Uzan, J. Cosmol. Astropart. Phys. 09 (2020) 020.
[18] M. Bojowald, Universe **6**, 125 (2020).
[19] M. Bojowald, S. Brahma, and D. h. Yeom, Phys. Rev. D **98**, 046015 (2018).
[20] M. Bojowald, Front. Phys. **3**, 33 (2015).
[21] E. T. Newman and A. I. Janis, J. Math. Phys. (N.Y.) **6**, 915 (1965).

[22] C. Liu, T. Zhu, Q. Wu, K. Jusufi, M. Jamil, M. Azreg-Ainou, and A. Wang, Phys. Rev. D **101**, 084001 (2020).
[23] F. Caravelli and L. Modesto, Classical Quantum Gravity **27**, 245022 (2010).
[24] M. Azreg-Ainou, Classical Quantum Gravity **28**, 148001 (2011).
[25] M. Bouhmadi-López, S. Brahma, C. Y. Chen, P. Chen, and D. h. Yeom, Phys. Dark Universe **30**, 100701 (2020).
[26] K. Akiyama *et al.* (Event Horizon Telescope Collaboration), Astrophys. J. **875**, L1 (2019).
[27] M. Azreg-Aïnou, Phys. Rev. D **90**, 064041 (2014).
[28] See Supplemental Material at http://link.aps.org/supplemental/10.1103/PhysRevLett.126.181301 for a detailed derivation of the rLQGO metric, its asymptotic expression, the Arnowitt-Deser-Misner mass, the removal of closed timelike curves, the geodesic equations, and the Klein-Gordon equation, which includes Refs. [29–35].
[29] M. Azreg-Aïnou, Eur. Phys. J. C **74**, 2865 (2014).
[30] H. C. D. L. Junior, L. C. B. Crispino, P. V. P. Cunha, and C. A. R. Herdeiro, Eur. Phys. J. C **80**, 1036 (2020).
[31] R. M. Wald, *General Relativity* (University of Chicago Press, Chicago, 1984).
[32] R. Shaikh, Phys. Rev. D **98**, 024044 (2018).
[33] M. Amir, K. Jusufi, A. Banerjee, and S. Hansraj, Classical Quantum Gravity **36**, 215007 (2019).
[34] D. J. Raine and E. G. Thomas, *Black Holes: An Introduction* (Imperial College Press, London, 2010).
[35] B. Carter, Commun. Math. Phys. **10**, 280 (1968).
[36] W. C. Gan, N. O. Santos, F. W. Shu, and A. Wang, Phys. Rev. D **102**, 124030 (2020).
[37] S. Hossenfelder, L. Modesto, and I. Prémont-Schwarz, Phys. Rev. D **81**, 044036 (2010).
[38] P. Bueno, P. A. Cano, F. Goelen, T. Hertog, and B. Vercnocke, Phys. Rev. D **97**, 024040 (2018).
[39] C. Y. Chen and P. Chen, Phys. Rev. D **100**, 104054 (2019).
[40] R. Shaikh, Phys. Rev. D **100**, 024028 (2019).
[41] S. Brahma, C. Y. Chen, and D. h. Yeom (to be published).
[42] K. Akiyama *et al.* (Event Horizon Telescope Collaboration), Astrophys. J. **875**, L6 (2019).
[43] D. Psaltis *et al.* (EHT Collaboration), Phys. Rev. Lett. **125**, 141104 (2020).
[44] J. G. Williams, S. G. Turyshev, and D. H. Boggs, Phys. Rev. Lett. **93**, 261101 (2004).
[45] F. Tamburini, B. Thidé, and M. Della Valle, Mon. Not. R. Astron. Soc. **492**, L22 (2020).
[46] R. Craig Walker, P. E. Hardee, F. B. Davies, C. Ly, and W. Junor, Astrophys. J. **855**, 128 (2018).
[47] H. M. Haggard and C. Rovelli, Phys. Rev. D **92**, 104020 (2015).